JB Journals.ASM.org

Identification of New Residues Involved in Intramolecular Signal Transmission in a Prokaryotic Transcriptional Repressor

Carlos Molina-Santiago,[a] Abdelali Daddaoua,[a] Sandy Fillet,[a]* Tino Krell,[a] Bertrand Morel,[b] Estrella Duque,[a] Juan L. Ramos[a,c]

Department of Environmental Protection, Consejo Superior de Investigaciones Científicas, Granada, Spain[a]; Department of Physical-Chemistry and Institute of Biotechnology, Faculty of Sciences, University of Granada, Campus de Fuentenueva, Granada, Spain[b]; Abengoa Research, Campus Palmas Altas, Seville, Spain[c]

TtgV is a member of the IclR family of transcriptional regulators. This regulator controls its own expression and that of the *ttgGHI* operon, which encodes an RND efflux pump. TtgV has two domains: a GAF-like domain harboring the effector-binding pocket and a helix-turn-helix (HTH) DNA-binding domain, which are linked by a long extended helix. When TtgV is bound to DNA, a kink at residue 86 in the extended helix gives rise to 2 helices. TtgV contacts DNA mainly through a canonical recognition helix, but its three-dimensional structure bound to DNA revealed that two residues, R19 and S35, outside the HTH motif, directly contact DNA. Effector binding to TtgV releases it from DNA; when this occurs, the kink at Q86 is lost and residues R19 and S35 are displaced due to the reorganization of the turn involving residues G44 and P46. Mutants of TtgV were generated at positions 19, 35, 44, 46, and 86 by site-directed mutagenesis to further analyze their role. Mutant proteins were purified to homogeneity, and differential scanning calorimetry (DSC) studies revealed that all mutants, except the Q86N mutant, unfold in a single event, suggesting conservation of the three-dimensional organization. All mutant variants bound effectors with an affinity similar to that of the parental protein. R19A, S35A, G44A, Q86N, and Q86E mutants did not bind DNA. The Q86A mutant was able to bind to DNA but was only partially released from its target operator in response to effectors. These results are discussed in the context of intramolecular signal transmission from the effector binding pocket to the DNA binding domain.

Efflux pumps of the RND (resistance-nodulation-cell division) family mediate resistance and tolerance to a wide range of toxic molecules in Gram-negative bacteria. *Pseudomonas putida* DOT-T1E exhibits an extremely high tolerance to solvents due to the synergic action of three RND efflux pumps (1, 2), called TtgABC, TtgDEF, and TtgGHI, that expel organic solvents from the cells (3–8). The TtgGHI efflux pump is, from a quantitative point of view, the main toluene extrusion element in DOT-T1E (3, 9), and the control of the expression of this efflux pump is mediated by the *ttgV* gene product.

The *ttgV* gene and the *ttgGHI* operon are transcribed divergently, and their promoters overlap, so that binding of TtgV to its operator represses the transcription from its own promoter and that of the *ttgG* promoter (10). TtgV, a member of the IclR family of regulators (11), binds to a number of aromatic compounds known as effectors, including 1-naphthol and indole (10, 12). TtgV was previously purified to homogeneity, and a number of biochemical assays revealed that it is a tetramer (12). The three-dimensional structures of TtgV in its apoprotein form and when bound to its target DNA operator were solved by Lu et al. (13). The cocrystal protein-DNA complex revealed that the numerous interactions between TtgV and DNA induced significant distortions within the DNA major groove, which lead to a curvature of 60° at the promoter region (Fig. 1A) (13). A number of direct interactions between DNA and TtgV take place through amino acid residues R47, T49, R52, and L57, which form part of a helix-turn-helix motif (HTH) (13, 14). The TtgV/operator cocrystal structure also revealed that amino acids S35 and R19, both located outside the HTH motif (Fig. 1) (13, 14), established direct contacts with DNA, although their role in DNA binding was not defined.

Lu et al. (13) showed that in its apoprotein form, the two domains of TtgV are aligned through a straight helix; however, when TtgV is bound to DNA, a 90° angle is introduced (Fig. 1), breaking the single helix into two smaller helices. This bend occurs at residue Q86 located within the connecting helix (13). Apart from being the residue at which the helix kink is introduced, Q86 plays also a central role in establishing intradimer contacts. As shown in Fig. 1D, Q86 side chains from the two monomers of the dimer establish two hydrogen bonds; DNA binding causes these bonds to break. Comparison of the three-dimensional structures of apoproteins TtgV and TtgV bound to DNA revealed that the turn of the HTH motif facilitates the interactions between S35, R19, and DNA and that residues G44 and P46 within this turn region are involved in the process (Fig. 1). This study aimed to determine the role of residues 19, 35, 44, 46, and 86 in TtgV regulator function. Thus, mutants in these residues were characterized physicochemically in the presence of 1-naphthol and DNA to gauge their effect on effector and DNA binding.

MATERIALS AND METHODS

Site-directed mutagenesis. TtgV mutants were generated by amplification of the *ttgV* gene in plasmid pET28b:TtgV using *Pfu* turbo DNA polymerase (Stratagene) and 39-mer overlapping primers that incorporated

Received 21 May 2013 **Accepted** 9 November 2013

Published ahead of print 15 November 2013

Address correspondence to Juan L. Ramos, juan.ramos@research.abengoa.com.

* Present address: Sandy Fillet, Neuron Pharma, Granada, Spain.

C.M.-S. and A.D. contributed equally to this work.

Supplemental material for this article may be found at http://dx.doi.org/10.1128/JB.00589-13.

doi:10.1128/JB.00589-13

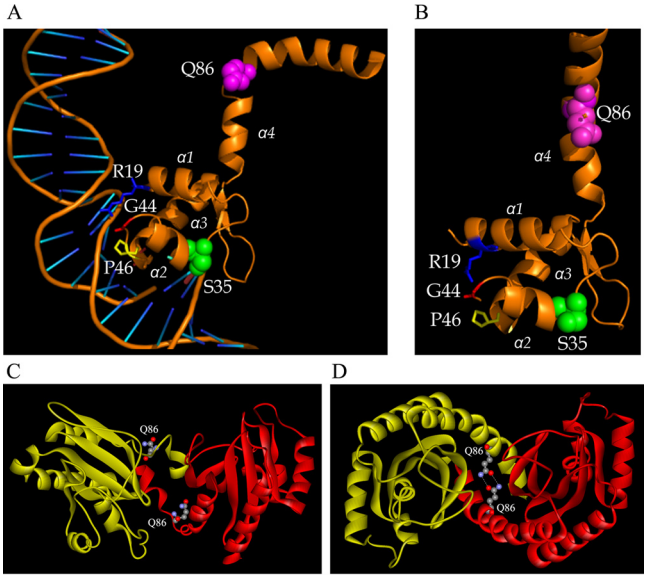

FIG 1 Structural changes induced by the binding of TtgV to DNA. Structure of the TtgV DNA binding domain and the flanking helix α4 in the DNA-bound state (A) and ligand-free state (B). View down the 2-fold axis of DNA-bound (C) and ligand-free (D) TtgV. Glutamine 86 is highlighted. In the DNA-free state, the residues from each monomer of the dimer establish two hydrogen bonds. For clarity purposes, the DNA-binding domain is not shown. The PDB ID of the ligand-free form of TtgV is 2XRN, and that of the DNA-bound form is 2XRO.

appropriate mismatches to introduce the desired mutations (15). The PCR product corresponding to the full plasmid with the expected mutations was digested with DpnI and transformed into *Escherichia coli* BL21(DE3). The TtgV mutant proteins were produced and purified to homogeneity using the protocol described by Fillet et al. (14).

Isothermal titration calorimetry. Microcalorimetric experiments were carried out at 25°C using a Valerian-Plotnikov (VP)-microcalorimeter (Microcal, Amherst, MA). Protein and substrates were dialyzed against 25 mM Tris-acetate (pH 8), 100 mM NaCl, 8 mM magnesium acetate, 1 mM dithiothreitol (DTT), and 10% (vol/vol) glycerol. Typically, a 4.8-μl aliquot of a 500 μM 1-naphthol solution, serving as an effector, was injected into a 40 μM solution of TtgV (1.2 ml) or the corresponding mutants. All data were corrected using the heat changes arising from injection of the effector into buffer. Data were analyzed using the "one-binding site model" of the MicroCal version of Origin. Titration curves were fitted by a nonlinear least-squares method to a function for the binding of one molecule of substrate to one molecule of target protein. The parameters ΔH (reaction enthalpy) and K_A (binding constant, $K_A = 1/K_D$, where K_D is the equilibrium dissociation constant) were determined from the fit of the curve. The changes in free energy (ΔG) and in entropy (ΔS) were calculated from the values of K_A and ΔH, using the equation $\Delta G = -RT \ln K_A = \Delta H - T\Delta S$, where R is the universal molar gas constant and T is the absolute temperature (16).

Differential scanning calorimetry. Differential scanning calorimetry experiments were carried out using a VP differential scanning calorimeter (DSC), a capillary-cell microcalorimeter from MicroCal (Northampton, MA), at a scan rate of 60°C/h from 5°C to 85°C. Protein samples were dialyzed for 48 h in 20 mM PIPES [piperazine-*N*,*N*′-bis(2-ethanesulfonic acid)], 8 mM magnesium acetate, 150 mM KCl, 1 mM Tris (2-carboxyethyl) phosphine (TCEP), pH 7.2. Dialyzed samples were centrifuged for 10 min at 14,000 × *g* in a cold room. Then, the concentration of the protein in solution was determined at 280 nm, using an extinction coefficient of 7,575 M^{-1} cm^{-1} (using the Protparam tool; Expasy). When indicated, naphthol was added to reach a final concentration of 33 or 250 μM, in the latter case to ensure that full saturation of the regulator was reached in each DSC scan.

Calorimetric cells (operating volume, 0.134 ml) were kept under an excess pressure of 60 lb/in^2 bar to prevent degassing during the scan. Several buffer-buffer baselines were obtained before each run with protein solution in order to ascertain proper equilibration of the instrument. Reheating was not performed, as previous studies on TtgV have proved that the denaturation of the protein leads to white precipitates and the unfolding process is therefore not reversible (17).

Circular dichroism. Protein samples were thawed and centrifuged at 14,000 × *g* for 10 min. Supernatant protein concentrations were determined by measuring absorbance and adjusted to a concentration of 40 μM. Naphthol was added from a 100-fold-concentrated stock solution to obtain final concentrations of 33 μM or 250 μM. Midpoint temperatures (T_m) values were obtained from the midpoint transition of the denaturation curves at 222 nm, and α-helix contents were calculated using the algorithm described by Luo and Baldwin (18).

EMSAs. For electrophoretic mobility shift assays (EMSAs), DNA fragments containing the *ttgGHI* promoter were amplified using pGG1 as a template with the primer pair 5′-NNNNNNGAATTCGTTCATATCTTTCCTCTGCG-3′and 5′-NNNNNNCTGCAGGGGGATTACCCGTAATGCAC-3′. Fragments were isolated from agarose gels and end labeled with [γ-^{32}P]deoxy-ATP using the T4 polynucleotide kinase. A 10-μl sample containing about 2 nM labeled DNA (1.5 × 10^4 cpm) was incubated with various concentrations of purified TtgV for 15 min in 10 μl of binding buffer (50 mM Tris-HCl [pH 7.5], 10 mM NaCl, 0.5 M magnesium acetate, 0.1 mM EDTA, 1 mM DTT, 5% [vol/vol] glycerol) containing 20 μg/ml of poly(dI-dC) and 200 μg/ml bovine serum albumin. The DNA-protein complexes were resolved by electrophoresis in 4% (wt/vol) nondenaturing polyacrylamide gels in 1× Tris-borate-EDTA buffer (TBE) as previously described (9, 19).

β-Galactosidase assays. Cultures were inoculated with bacterial cells from fresh LB agar plates and grown overnight at 30°C on LB medium with appropriate antibiotics. Cultures were diluted to an initial turbidity at 660 nm of 0.05 in the same medium supplemented or not with 1-naphthol (1 mM) dissolved in dimethyl sulfoxide (note that the latter did not interfere with the induction assays in this study). β-Galactosidase activity was determined in triplicate for permeabilized cells when cultures reached a turbidity at 660 nm of 0.5 (20). The results reported are the means of nine assays.

RESULTS

Residue Q86 is involved in the structural reorganization of TtgV in response to effectors influencing the stability of the protein. TtgV proteins with mutations in residues 86, 46, 44, 35, and 19 were generated by site-directed mutagenesis with the aim of studying the role of these residues in the repression function of the protein. At all positions, we replaced the corresponding residue by alanine. In addition, at position 86, which is located at the kink in the α-helix contacting both domains, we replaced Q by N and G to test the effect of the size of the lateral side chain residue and replaced Q by E to check the effect of the lateral side residue charge. The four mutant variants at residue 86 and the other four alanine mutants at residues 46, 44, 35, and 19 were purified as homogeneous proteins at concentrations of >10 mg/ml and were stable at 4°C. Circular dichroism (CD) analyses were carried out in the presence and in the absence of different concentrations of 1-naphthol. We found that all mutants, in the presence and in the absence of 33 μM and 250 μM naphthol, yielded similar CD results with α-helix percentages between 22.5 and 23.7% (see Fig. S1 in the supplemental material). To determine the stability of TtgV, we carried out DSC assays to establish the thermal unfolding of TtgV and its variants. TtgV unfolds in a single event with a T_m of 46.3°C

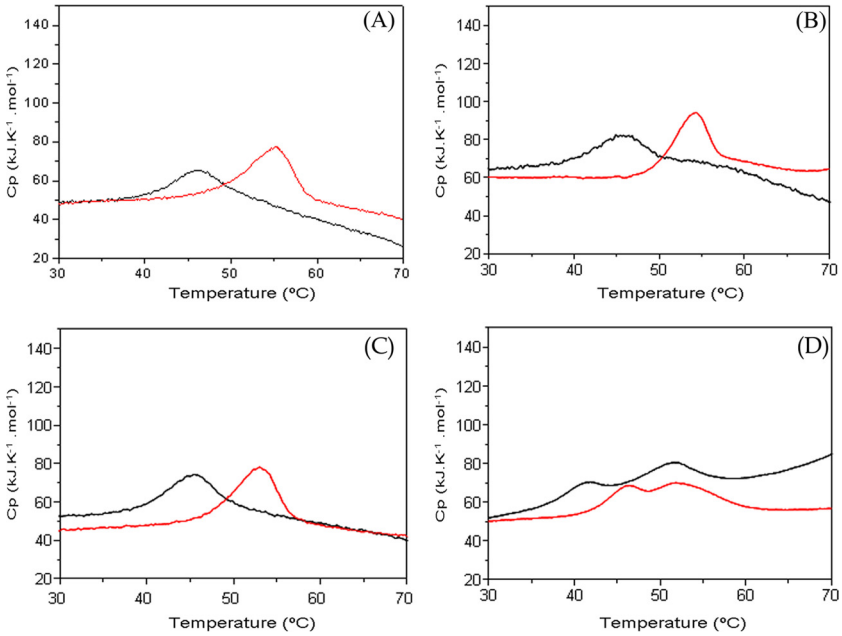

FIG 2 Effects of 1-naphthol on the thermal unfolding of TtgV and mutant variants: wild type (WT) (A) and R19A (B), Q86G (C), and Q86N (D) mutants. For all panels, the DSC experiments of the TtgV mutants were performed in the absence of effector (black line) and in the presence of 250 μM 1-naphthol (red line). Details of the assays are given in Materials and Methods.

(Fig. 2). Similar results were obtained with all mutants (Fig. 2 and Table 1; see Fig. S2 in the supplemental material), except for the Q86N mutant, which unfolds in two events, with T_m of 41°C and 52°C (Fig. 2D). We previously demonstrated that effector binding to TtgV leads to stabilization of the protein (17) and an increase in T_m of the wild type from 46.3°C to 55.2°C in the presence of 250 μM 1-naphthol (Fig. 2A). In the present study, we similarly observed that the addition of 1-naphthol stabilized all mutant proteins (Table 1). With the Q86N mutant, which unfolded in two events, the presence of 1-naphthol enhanced the stability of the unfolding event at the lower temperature (T_m increased from 41.4°C to 46.5°C). This suggests that in the Q86N mutant the effector binding domain corresponds to the domain that unfolds at the lower temperature.

TABLE 1 Thermodynamic parameters obtained by integration of the peak obtained from the DSC thermal unfolding assays[a]

TtgV protein	Naphthol[b]	T_m (°C)	ΔH_m (kJ · mol^{-1})
WT	−	46.30	177
	+	55.19	178
R19A mutant	−	46.43	147
	+	54.33	192
Q86A mutant	−	45.88	190
	+	52.87	225
Q86G mutant	−	45.57	205
	+	53.04	194
Q86N mutant	−	41.4	51.05
	−	51.33	111
	+	46.46	73.52
	+	51.83	122
Q86E mutant	−	45.72	157
	+	52.68	198
G44A mutant	−	49.62	110
	+	50.68	140
P46A mutant	−	47.23	190
	+	55.30	335

[a] Values are presented for each resolvable DSC profile peak.
[b] +, presence of 250 μM naphthol; −, no naphthol present.

Isothermal titration calorimetry (ITC) assays were then carried out to determine if the TtgV mutations affect effector binding. Significant heat changes were observed when 1-naphthol was added to the wild-type protein or any of the mutant proteins (Fig. 3). Titration of TtgV mutant proteins (40 μM) with 0.5 mM 1-naphthol produced large exothermic heat changes (Q86A mutant; Fig. 3B), confirming that the TtgV mutants recognized 1-naphthol. The wild-type TtgV protein bound 1-naphthol with an affinity of approximately 15 μM. The affinity of most TtgV mutants was in the range of 7 to 20 μM, although it should be noted that an increase in affinity for 1-naphthol was observed for the G44A (3.5 μM) (Table 2). Fitting of the integrated and dilution-corrected raw data with the "one binding site model" using Origin software (MicroCal) revealed that binding is, in general, driven by favorable enthalpy changes ($\Delta H = -7.55 \pm 0.38$ kcal/mol for G44A to -32.7 ± 4.7 kcal/mol for Q86E) and counterbalanced, in general, by unfavorable entropy changes.

To determine whether mutant proteins bind to DNA, we carried out EMSAs, which showed that Q86N and Q86E mutants were unable to bind DNA, whereas the Q86A and Q86G mutants behaved like the wild type (Fig. 4). In contrast to alanine and glycine, asparagine and glutamine side chains are able to form hydrogen bonds, and it is plausible that the differential capacity of the different Q86 mutants may be related to the establishment of

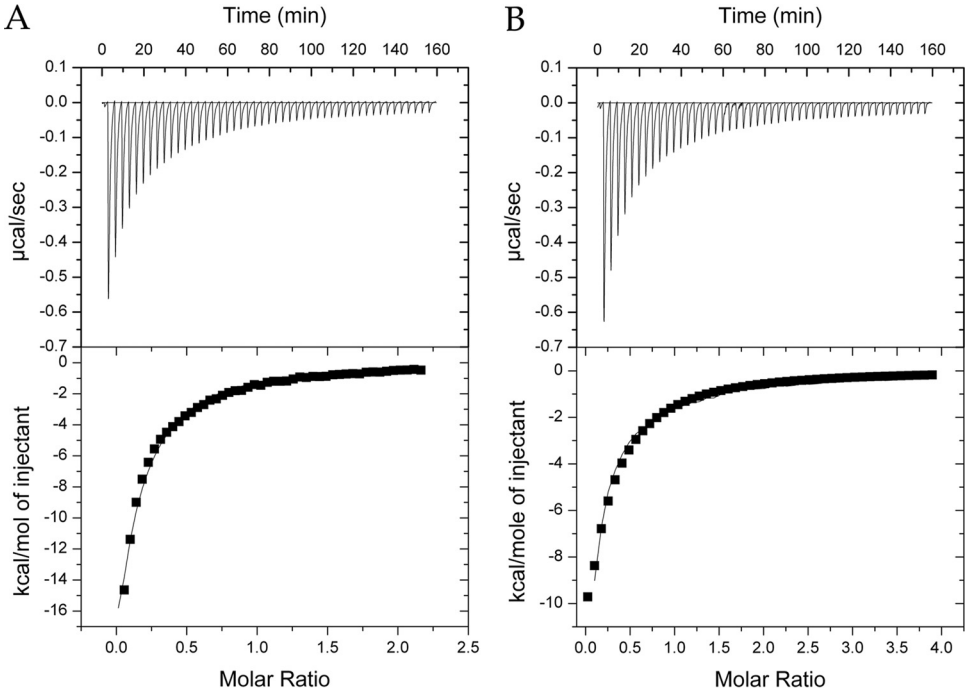

FIG 3 Microcalorimetric titration of TtgV with 1-naphthol. (Upper panels) Raw data for the injection of 4.8-μl aliquots of 0.5 mM 1-naphthol into 40 μM TtgV wild type (A) and Q86N mutant (B). (Lower panels) Integrated, dilution corrected, and protein concentration normalized peak areas of the raw data. Data were fitted using the "one binding site model" of MicroCal Origin.

hydrogen bonds with other amino acids. The inspection of the dimer interface of TtgV (13) revealed that the Q86 side chains interact, forming two hydrogen bonds. The introduction of a negatively charged Glu side chain instead of the neutral Gln into the center of the dimer interface is likely to create charge repulsion and structural alterations. Mutants at residues R19 and S35 failed to bind DNA, corroborating their role in DNA interactions as reported from the analysis of the TtgV/operator cocrystal structure (13). Mutations of G44 and P46 to alanine had a differential impact on the DNA binding capacity: while the P46A mutant was able to bind promoter DNA, the G44A mutant was devoid of DNA binding ability. When EMSAs of the mutant variants that bound DNA were carried out in the presence of 1-naphthol, all of them were released from the DNA (Fig. 4). This set of results indicated that in addition to residues in the HTH, which bind the operator, additional residues such as R19 and S35 are critical for DNA binding, mainly because the target operator is bent during binding, allowing alternate contact points.

TtgV mutant release from target DNA was analyzed using EMSA. TtgV release from DNA involves interaction of the regulator with the effector, as well as intramolecular signal transmission (Fig. 5). We found that the wild type and all mutants are released after effector binding according to a hyperbolic curve with increasing effector concentration. For the P46A mutant, we found that a concentration of 0.87 mM 1-naphthol was required to release 50% of the bound protein, which is a value comparable to that of the wild type. Interestingly, much higher 1-naphthol concentrations were necessary to trigger the release of the Q86A and Q86G mutants, demonstrating that the Q86 residue is key in the intramolecular signal transmission process.

***In vivo* behavior of TtgV mutants.** To test whether the TtgV mutants behaved *in vivo* as deduced from *in vitro* results, we used a fusion of P_{ttgG} to *lacZ* and introduced the *ttgV* wild-type gene or its mutant variants in *trans* in pBBR (14). Expression from P_{ttgG} was repressed *in vivo* by TtgV, and basal expression increased about 3-fold in response to 1-naphthol, in agreement with previous results (Table 3) (10). Q86A and Q86G mutants behaved like the wild type, as expected from the *in vitro* assays. Q86E, G44A,

TABLE 2 Thermodynamic parameters derived from the microcalorimetric titration of wild-type and mutant TtgV with 0.5 mM 1-naphthol

Protein	K_D (μM)	K_A (M^{-1})	ΔH (kcal · mol^{-1})	ΔG (kcal · mol^{-1})
WT	15.2 ± 1.9	(6.6 ± 0.5) × 10^4	−14.5 ± 0.49	−6.6 ± 0.04
Q86E mutant	10.2 ± 1.3	(9.8 ± 1.2) × 10^4	−32.7 ± 4.77	−6.7 ± 0.07
R19A mutant	8.0 ± 0.9	(12.5 ± 1.5) × 10^4	−22.4 ± 0.97	−6.8 ± 0.07
Q86G mutant	16.0 ± 0.2	(6.24 ± 4.3) × 10^4	−18.2 ± 0.56	−6.5 ± 0.01
Q86N mutant	6.6 ± 0.5	(15.2 ± 2.0) × 10^4	−6.5 ± 0.33	−7.1 ± 0.08
Q86A mutant	20.2 ± 1.3	(4.9 ± 0.3) × 10^4	−11.7 ± 0.36	−6.3 ± 0.04
S35A mutant	11.9 ± 0.5	(8.4 ± 0.4) × 10^4	−24.4 ± 0.43	−6.6 ± 0.02
P46A mutant	8.2 ± 0.7	(12.2 ± 1.1) × 10^4	−27.5 ± 0.85	−6.8 ± 0.04
G44A mutant	3.5 ± 0.6	(28.7 ± 5.3) × 10^4	−7.55 ± 0.38	−7.3 ± 0.1

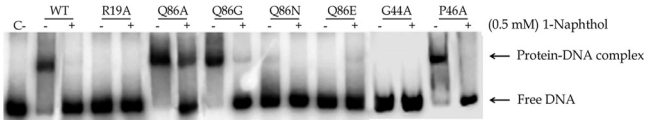

FIG 4 Interaction of TtgV and its mutant derivatives with *ttgGHI* promoter studied by EMSA. A DNA fragment (2 nM) comprising the 295-bp intergenic *ttgV-ttgG* region was incubated without (C−) and with wild-type or mutant TtgV in the absence (−) or in the presence (+) of 1-naphthol. The TtgV proteins were added to reach a concentration of 1 μM, and 1-naphthol was added to a final concentration of 2 mM.

R19A, and S35A mutants did not bind DNA, and consequently expression from P_{ttgG} was high regardless of the presence of 1-naphthol, in consonance with the *in vitro* results (Table 3).

DISCUSSION

The structure of the ligand-free TtgV regulator is composed of two domains that are connected by a long extended helix. Effector binding to the DNA-bound repressor causes major structural changes in which a 90° kink is introduced into this helix, altering the respective positions of the DNA- and effector-binding domains. These structural alterations trigger the release of the DNA-bound protein. Interestingly, the TtgV linker can be classified as glutamine-rich linker or Q-linker, initially described by Wootton and Drummond (21) as interdomain helices rich in glutamine and glutamate residues. There are a number of studies available that show that Q-linkers are important for efficient interdomain communication (22, 23). However, the functional basis for the existence and conservation of Q-linkers is poorly understood.

Here, we show that mutation of Q86 of the TtgV Q-linker has multiple consequences on protein function. This is illustrated by the mutant in which Q86 was replaced by asparagine. Although this amino acid replacement is highly conservative, DSC data show that the mutant unfolds in two separate events instead of a single event for the native protein (Table 1). The same mutant had an increased affinity for 1-naphthol, approximately 3-fold (Table 3), and EMSA data (Fig. 5) showed that the replacement of Q86 renders the protein less efficient in its capacity to mediate its dissociation in response to 1-naphthol.

A plausible structural reason for the central role of Q86 may be its involvement in establishing two intradimer hydrogen bonds (Fig. 1). DNA binding would break these bonds and trigger the introduction of a kink in the Q-helix with its apex on Q86. For the four Q86 mutants analyzed, none of the substituent amino acids is likely to form intradimer hydrogen bonds (the two asparagine side chains are too far removed for mutual interaction), and it can be suggested that the pronounced effects observed for these mutants may be caused by the absence of hydrogen bonds formed between the Q86 substituents.

Parallels exist to the NarL response regulator, which was also shown to possess a Q-linker. It was shown that NarL phosphorylation causes the separation of both domains caused by a hinge bending of the Q-linker allowing for the otherwise hindered DNA binding (24). Combined data suggest that a functional feature characteristic of Q-linkers may be their capacity to allow kink formation and consequently domain separation.

Q86 is not the only key residue in the TtgV Q-linker. In previous work, we have shown that the formation of an intramonomer salt bridge between R98 and E102 was essential to interdomain communication (17). This salt bridge is formed only in the DNA-

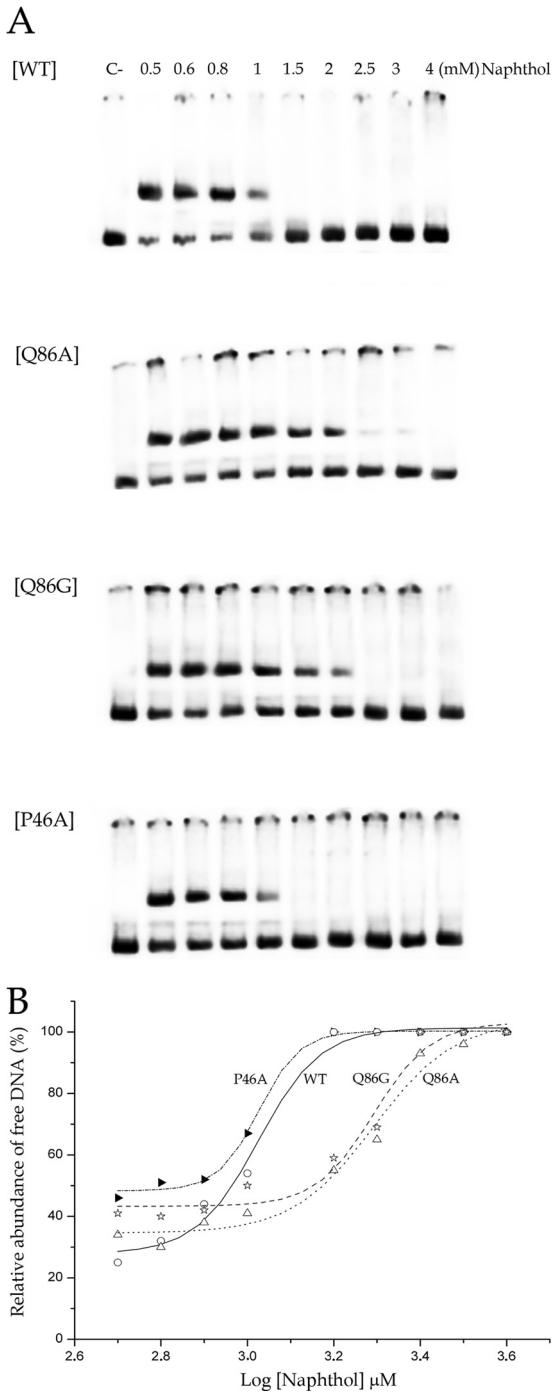

FIG 5 Release of wild-type TtgV and mutants bound to the intergenic *ttgV-ttgG* region in the presence of increasing concentrations of 1-naphthol. EMSAs were carried out as described for Fig. 4, except that different concentrations of 1-naphthol were used, and densitometric analyses were performed (using Quantity One software) to determine the amount of DNA released in the presence of increasing concentrations of 1-naphthol with respect to the total shifted DNA in the absence of ligand. (A) EMSAs were carried out with 2 nM the indicated *ttgV-ttgG* intergenic region (295-bp fragment) (lane C) and 1 μM wild-type or mutant TtgV proteins incubated with increasing concentrations of 1-naphthol (0.5, 0.6, 0.8, 1, 1.5, 2, 2.5, 3, and 4 mM). (B) Representation of the relative abundance of free DNA versus the concentration (log) of 1-naphthol. MicroCal Origin software was used to calculate the relative abundance of free DNA (%) and the EC_{50} of each protein, defined as the ligand concentration for which 50% of the shifted DNA is released.

TABLE 3 Regulated expression from the P_{ttgG} promoter mediated by TtgV or its mutant variants

Regulator	Activity (Miller units)	
	Without 1-naphthol	With 1-naphthol
None	3,755 ± 280	3,980 ± 250
TtgV	1,325 ± 120	3,900 ± 220
TtgVQ86A	2,115 ± 120	3,500 ± 150
TtgVQ86G	1,355 ± 125	3,660 ± 200
TtgVQ86E	3,830 ± 260	4,120 ± 90
TtgVS35A	3,890 ± 300	4,500 ± 170
TtgVR19G	4,240 ± 250	4,225 ± 205
TtgVG44A	4,250 ± 160	4,230 ± 225

bound state and is dissolved in the ligand-free form of TtgV (13). In analogy to the Q86 mutant, the mutation of both R98 and E102 caused the two domains to unfold in a sequential manner (17).

Two other groups of residues were analyzed in this work: G44 and P46, which form part of the HTH turn, and R19 and S35, which are located outside the HTH motif. The TtgV structure shows that the loop harboring G44 and P46 is the part of the structure farthest removed from the effector binding site. However, mutation of both residues significantly influenced 1-naphthol affinity (Table 2) and also increased the thermal stability of the protein by approximately 1°C (P46A) and 3°C (G44A). However, the replacement of both residues by alanine had different effects on their DNA-binding capacity. Whereas the replacement of P46 by A had little effect on the protein, the G44A mutant was unable to bind to DNA. Both residues are located on a very sharp turn connecting both helices of the HTH motif, and an amino acid with elevated conformational freedom such as glycine may be required at this position to guarantee the formation of this turn.

The main determinants for DNA binding are usually located within the HTH motif. The TtgV structure shows that R19 and S35 interact directly with neighboring DNA phosphate moieties. Here, we show that mutation of two residues that are located earlier in the protein sequence than the HTH motif abolished DNA binding. This feature may be due to the fact that TtgV binding causes strong DNA distortion, enabling other contacts with DNA.

TtgV belongs to the IclR family of transcriptional regulators (11), and we have aligned the 50 most similar members of the IclR family to TtgV to determine whether the residues at positions 19, 35, 44, 46, and 86 were conserved and if they played a general role in this family or, if not conserved, whether they played a more specific role in TtgV. The alignment revealed (see Fig. S3 in the supplemental material) that the residues equivalent to S35 (50 of 50), R19 (49 of 50), and P46 (46 of 50) were very conserved, whereas at position G44 and Q86 there was a low degree of conservation. This suggests that S35 and R19 could also play a role in DNA binding in other regulators of this family. Our results also reveal that residues 44 and 86 likely play specific roles in TtgV as a repressor.

In summary, we identify here a key glutamine residue in a Q-linker of an IclR-family transcriptional regulator and provide evidence that amino acids outside the HTH are essential for DNA binding.

ACKNOWLEDGMENTS

Work in our laboratory was supported by the Fondo Social Europeo and Fondos Feder from the European Union through grants of the Junta de Andalucía (CVI-7391) and the Ministry of Science and Innovation (BIO 2010-17227 and BIO2011-12776) awarded to the CSIC.

We thank M. M. Fandila for secretarial assistance and Ben Pakuts for critical reading of the manuscript.

REFERENCES

1. **Ramos JL, Duque E, Huertas MJ, Haidour A.** 1995. Isolation and expansion of the catabolic potential of a *Pseudomonas putida* strain able to grow in the presence of high concentrations of aromatic hydrocarbons. J. Bacteriol. **177:**3911–3916.
2. **Duque E, Segura A, Mosqueda G, Ramos JL.** 2001. Global and cognate regulators control the expression of the organic solvent efflux pumps TtgABC and TtgDEF of *Pseudomonas putida*. Mol. Microbiol. **39:**1100–1106. http://dx.doi.org/10.1046/j.1365-2958.2001.02310.x.
3. **Rojas A, Duque E, Mosqueda G, Golden G, Hurtado A, Ramos JL, Segura A.** 2001. Three efflux pumps are required to provide efficient tolerance to toluene in *Pseudomonas putida* DOT-T1E. J. Bacteriol. **183:**3967–3973. http://dx.doi.org/10.1128/JB.183.13.3967-3973.2001.
4. **Ramos JL, Duque E, Godoy P, Segura A.** 1998. Efflux pumps involved in toluene tolerance in *Pseudomonas putida* DOT-T1E. J. Bacteriol. **180:**3323–3329.
5. **Ramos JL, Duque E, Gallegos MT, Godoy P, Ramos-Gonzalez MI, Rojas A, Teran W, Segura A.** 2002. Mechanisms of solvent tolerance in gram-negative bacteria. Annu. Rev. Microbiol. **56:**743–768. http://dx.doi.org/10.1146/annurev.micro.56.012302.161038.
6. **Isken S, de Bont JA.** 1996. Active efflux of toluene in a solvent-resistant bacterium. J. Bacteriol. **178:**6056–6058.
7. **Kieboom J, Dennis JJ, de Bont JA, Zylstra GJ.** 1998. Identification and molecular characterization of an efflux pump involved in *Pseudomonas putida* S12 solvent tolerance. J. Biol. Chem. **273:**85–91. http://dx.doi.org/10.1074/jbc.273.1.85.
8. **Fernández M, Niqui-Arroyo JL, Conde S, Ramos JL, Duque E.** 2012. Enhanced tolerance to naphthalene and enhanced rhizoremediation performance for *Pseudomonas putida* KT2440 via the NAH7 catabolic plasmid. Appl. Environ. Microbiol. **78:**5104–5110. http://dx.doi.org/10.1128/AEM.00619-12.
9. **Rojas A, Segura A, Guazzaroni ME, Terán W, Hurtado A, Gallegos MT, Ramos JL.** 2003. *In vivo* and *in vitro* evidence that TtgV is the specific regulator of the TtgGHI multidrug and solvent efflux pump of *Pseudomonas putida*. J. Bacteriol. **185:**4755–4763. http://dx.doi.org/10.1128/JB.185.16.4755-4763.2003.
10. **Guazzaroni ME, Terán W, Zhang X, Gallegos MT, Ramos JL.** 2004. TtgV bound to a complex operator site represses transcription of the promoter for the multidrug and solvent extrusion TtgGHI pump. J. Bacteriol. **186:**2921–2927. http://dx.doi.org/10.1128/JB.186.10.2921-2927.2004.
11. **Molina-Henares AJ, Krell T, Eugenia Guazzaroni M, Segura A, Ramos JL.** 2006. Members of the IclR family of bacterial transcriptional regulators function as activators and/or repressors. FEMS Microbiol. Rev. **30:**157–186. http://dx.doi.org/10.1111/j.1574-6976.2005.00008.x.
12. **Guazzaroni ME, Krell T, Felipe A, Ruiz R, Meng C, Zhang X, Gallegos MT, Ramos JL.** 2005. The multidrug efflux regulator TtgV recognizes a wide range of structurally different effectors in solution and complexed with target DNA: evidence from isothermal titration calorimetry. J. Biol. Chem. **280:**20887–20893. http://dx.doi.org/10.1074/jbc.M500783200.
13. **Lu D, Fillet S, Meng C, Alguel Y, Kloppsteck P, Bergeron J, Krell T, Gallegos MT, Ramos J, Zhang X.** 2010. Crystal structure of TtgV in complex with its DNA operator reveals a general model for cooperative DNA binding of tetrameric gene regulators. Genes Dev. **24:**2556–2565. http://dx.doi.org/10.1101/gad.603510.
14. **Fillet S, Velez M, Lu D, Zhang X, Gallegos MT, Ramos JL.** 2009. TtgV represses two different promoters by recognizing different sequences. J. Bacteriol. **191:**1901–1909. http://dx.doi.org/10.1128/JB.01504-08.
15. **Daniels C, Daddaoua A, Lu D, Zhang X, Ramos JL.** 2010. Domain cross-talk during effector binding to the multidrug binding TtgR regulator. J. Biol. Chem. **285:**21372–21381. http://dx.doi.org/10.1074/jbc.M110.113282.
16. **Krell T.** 2008. Microcalorimetry: a response to challenges in modern biotechnology. Microb. Biotechnol. **1:**126–136. http://dx.doi.org/10.1111/j.1751-7915.2007.00013.x.
17. **Fillet S, Krell T, Morel B, Lu D, Zhang X, Ramos JL.** 2011. Intramolecular signal transmission in a tetrameric repressor of the IclR family.

Proc. Natl. Acad. Sci. U. S. A. **108:**15372–15377. http://dx.doi.org/10.1073/pnas.1018894108.
18. **Luo P, Baldwin RL.** 1997. Mechanism of helix induction by trifluoroethanol: a framework for extrapolating the helix-forming properties of peptides from trifluoroethanol/water mixtures back to water. Biochemistry **36:**8413–8421. http://dx.doi.org/10.1021/bi9707133.
19. **Sasse J, Gallagher SR.** 2004. Staining proteins in gels. Curr. Protoc. Immunol. **Chapter 8:**Unit 8.9. http://dx.doi.org/10.1002/0471142735.im0809s58.
20. **Miller JH.** 1972. Experiments in molecular biology. Cold Spring Harbor Laboratory Press, Cold Spring Harbor, NY.
21. **Wootton JC, Drummond MH.** 1989. The Q-linker: a class of interdomain sequences found in bacterial multidomain regulatory proteins. Protein Eng. **2:**535–543. http://dx.doi.org/10.1093/protein/2.7.535.
22. **Mattison K, Oropeza R, Kenney LJ.** 2002. The linker region plays an important role in the interdomain communication of the response regulator OmpR. J. Biol. Chem. **277:**32714–32721. http://dx.doi.org/10.1074/jbc.M204122200.
23. **Walthers D, Tran VK, Kenney LJ.** 2003. Interdomain linkers of homologous response regulators determine their mechanism of action. J. Bacteriol. **185:**317–324. http://dx.doi.org/10.1128/JB.185.1.317-324.2003.
24. **Zhang JH, Xiao G, Gunsalus RP, Hubbell WL.** 2003. Phosphorylation triggers domain separation in the DNA binding response regulator NarL. Biochemistry **42:**2552–2559. http://dx.doi.org/10.1021/bi0272205.